Journal of
Marine Science and Engineering

MDPI

Article

Model Development and Hindcast Simulations of NOAA's Gulf of Maine Operational Forecast System

Zizang Yang [1,*], Philip Richardson [1], Yi Chen [2], John G. W. Kelley [1], Edward Myers [1], Frank Aikman III [1], Machuan Peng [3] and Aijun Zhang [3]

1 NOAA/National Ocean Service/Coast Survey Development Laboratory, 1315 East-West Highway, Silver Spring, MD 20910, USA; phil.richardson@noaa.gov (P.R.); john.kelley@noaa.gov (J.G.W.K.); edward.myers@noaa.gov (E.M.); frank.aikman@noaa.gov (F.A.)
2 Earth Resources Technology (ERT) Inc., 6100 Frost Place, Suite A, Laurel, MD 20707, USA; yi.chen@noaa.gov
3 NOAA/National Ocean Service/Center for Operational Oceanographic Products and Services, 1305 East-West Highway, Silver Spring, MD 20910, USA; machuan.peng@noaa.gov (M.P.); aijun.zhang@noaa.gov (A.Z.)
* Correspondence: zizang.yang@noaa.gov; Tel.: +1-301-713-2809

Academic Editor: Richard Signell
Received: 18 July 2016; Accepted: 24 October 2016; Published: 17 November 2016

Abstract: The National Ocean Service (NOS) of National Oceanic and Atmospheric Administration is developing an operational nowcast/forecast system for the Gulf of Maine (GoMOFS). The system aims to produce real-time nowcasts and short-range forecast guidance for water levels, 3-dimensional currents, water temperature, and salinity over the broad GoM region. GoMOFS will be implemented using the Regional Ocean Model System (ROMS). This paper describes the system setup and results from a one-year (2012) hindcast simulation. The hindcast performance was evaluated using the NOS standard skill assessment software. The results indicate favorable agreement between observations and model forecasts. The root-mean-squared errors are about 0.12 m for water level, less than 1.5 °C for temperature, less than 1.5 psu for salinity, and less than 0.2 m/s for currents. It is anticipated to complete the system development and the transition into operations in fiscal year 2017.

Keywords: Gulf of Maine; operational nowcast and forecast system; hydrodynamics; ROMS; water level; currents; water temperature; and salinity

1. Introduction

The Gulf of Maine (GoM) is a semi-enclosed coastal basin located along the coastline of the northeastern U.S. (Figure 1). It is surrounded by the New England coast to the west and to the north. It is adjacent to the Bay of Fundy (BF) to the northeast and is bounded by the coast of Nova Scotia to the east. To the south, the Gulf water communicates with the open ocean through a series of shoals, banks and channels, such as Nantucket Shoals (NS), the Great South Channel (GSC), Georges Bank (GB), the Northeast Channel (NEC), Brown Bank (BB), and the Cape Sable Channel (CSC).

The GOM/GB system demonstrates a broad variety of physical oceanography phenomena such as a complicated circulation system, intense tidal currents, fronts, internal tides, etc. Baroclinic hydrography, barotropic tidal dynamics, and meteorological factors are responsible for incurring their existence and modulating of their intensity. Their relative significance varies spatially as well as seasonally [1–5].

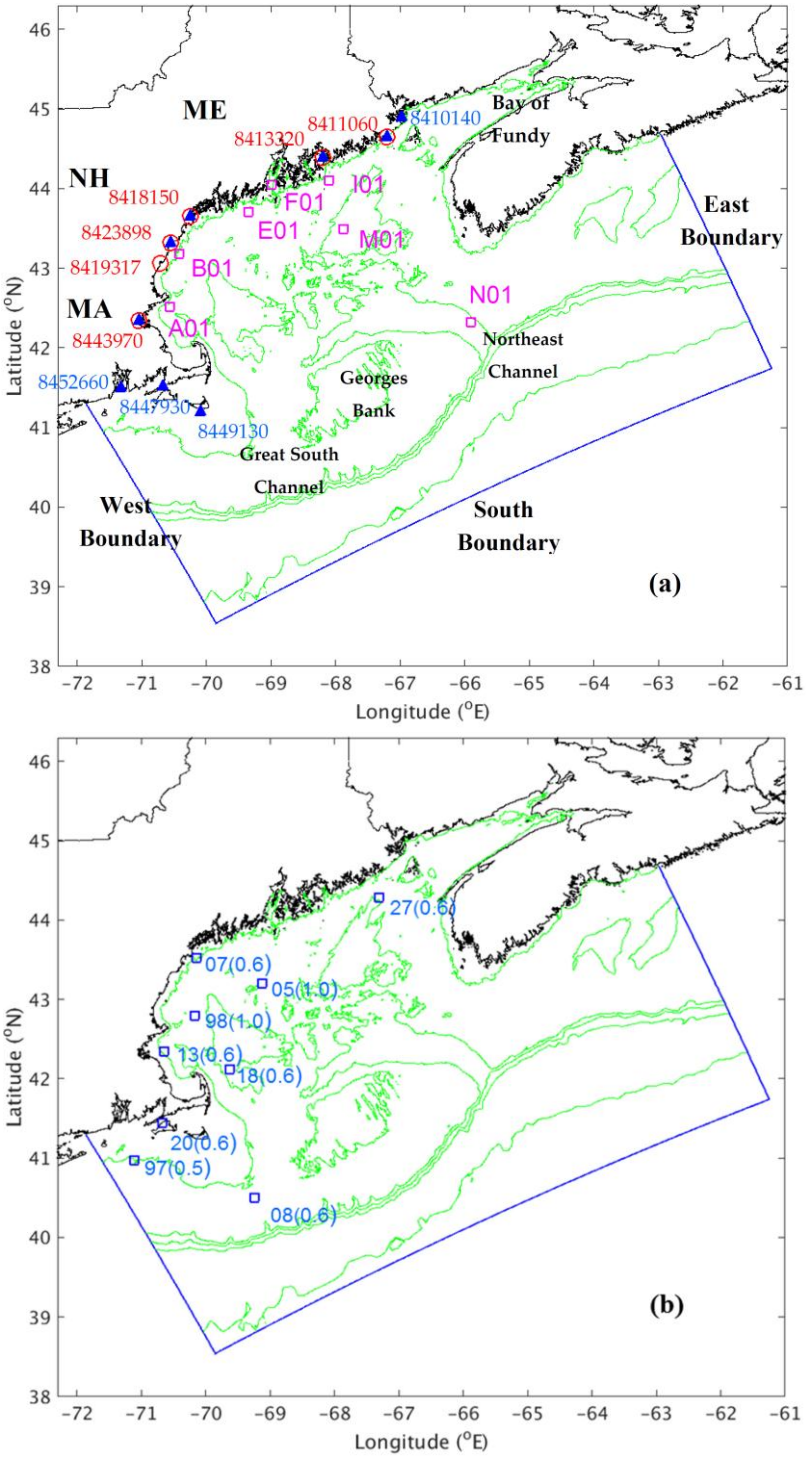

Figure 1. Map of the Gulf of Maine (GoM)/Georges Bank (GB) region and the GoMOFS model domain. Green lines represent the 50, 200, 500, 1000, and 3000-m isobaths. Blue lines denote the three open ocean boundaries of the model domain. (**a**) Map of observation stations: the CO-OPS water level stations (red circles) and water temperature stations (filled blue triangles), and the NeraCOOS buoys (magenta squares). The station IDs are labeled near the location markers. The measurement depths of the CO-OPS stations are 3.3 m (8410140), 2.4 m (8411060), 2.9 m (8413320), 4.9 m (8418150), 3.3 m (8419317), 2.9 m (8443970), 2.0 m (8447930), 1.2 m (8449130), and 1.8 m (8452660). The NeraCOOS depths are listed in Table 1; (**b**) Map of NDBC buoy stations. The station IDs are labeled near the location marks. Three leading digits "440" of each ID number are omitted for the clarity of illustration. The numbers in the parentheses following the IDs represent the measurement depths (in meters) relative to the sea surface.

The area is well known for its significant tidal fields. The tidal range is greater than 3 m along the northern and western coast and over 5 m in the BF. The tidal currents are as high as 0.5 to 1 m/s over the NS and GB. The tidal dynamics are heavily involved in forming the circulation, fronts, etc. [6]. Within the Gulf, tides are forced by ocean tides along the shelf break. Five tidal constituents, M_2, S_2, N_2, K_1, and O_1, account for 94% of the total tidal potential energy, while the M_2 constituent contributes over 80% of the total energy [7].

Researchers have explored the hydrodynamics of the area using various types of numerical models, such as the finite difference [8–10], finite element [4,11], and finite volume [12] models. Greenberg [8] and Naimie et al. [4] investigated the tidal dynamics of the M_2 astronomical constituent. Using the ADvanced CIRCulation (ADCIRC) model (ADCIRC), Yang and Myers [11] investigated the pathway and intensity of the barotropic M_2 tidal energy flux. Chen et al. [12] studied both barotropic and internal tidal dynamics in the region using the Finite Volume Coastal Ocean Model (FVCOM).

Several of the numerical studies focused on investigating the three-dimensional (3-D) hydrodynamics of the area. Naimie and Lynch [4] studied summer season stratification in the GB area using the unstructured-grid finite element model QUODDY. Chen et al. [9] used the modified Princeton Ocean Model (ECOM-si) to investigate the dynamics of the tidal currents rectifications and its impact on the formation of upwelling in the GB region. Xue et al. [5] simulated the seasonal circulations using the Princeton Ocean Model (POM). Gangopadhyay et al. [13] developed a multiscale feature model to study the characteristic physical circulation features. To support the Gulf of Maine Ocean Observing System (GoMOOS) operations, Xue et al. [10] developed the POM-based nowcasts/forecast system to produce real-time, 3-D distribution of circulation and water properties. More recently, Wilkin et al. [14] developed the data-assimilative "Doppio" real-time and reanalysis ROMS system to make the forecast of hydrodynamics for the broad Mid-Atlantic Bight and the GoM regions.

The National Ocean Service (NOS) of National Oceanic and Atmospheric Administration (NOAA) has recently been working on developing an operational oceanographic nowcast/forecast system for the Gulf of Maine (GoMOFS). The GoMOFS aims to produce real-time nowcast and short-range forecast guidance for water levels, 3-dimensional currents, water temperature, and salinity over the broad GoM region. It will support the GoM harmful algal bloom (HAB) forecast, marine navigation, emergency response, and the environmental management communities.

The GoMOFS uses the Regional Ocean Model System (ROMS) [15] as the hydrodynamic model. In developing the GoMOFS, we conducted a one-year hindcast simulation for the year of 2012 and evaluated the model performance using the NOS standard skill assessment software [16].

This article describes the model setup and skill assessment results of the hindcast simulation. It is organized as follows. This section reviews the general hydrodynamics in the Gulf, previous numerical studies, and NOAA's initiative in developing the GoMOFS. Section 2 describes the model setup of the 2012 hindcast simulation. Section 3 describes the observed data used for the skill assessment. Section 4 presents the model results. Section 5 describes the skill assessment results. Section 6 states the conclusion and summery.

2. Model Setup

The GoMOFS model has a nearly rectangular domain that goes from the eastern Long Island Sound in the west to the shelf of Nova Scotia in the east and extends to the deep ocean outside of the shelfbreak (see Figure 1). It has an orthogonal model grid with horizontal dimensions of 1177 by 776 and a uniform spatial resolution of 700 m. The grid resolved major coastal embayments including Cape Cod Bay, Boston Harbor, Casco Bay, Penobscot Bay, and the Bay of Fundy. However, the 700-m resolution prohibits the model from resolving small scale coastal features such as navigation channels and river courses, e.g., the Cape Cod Canal. The grid has three open ocean boundaries (see the blue lines in Figure 1): the western boundary in the western Long Island Sound, the southern boundary outside the shelfbreak to the southeast of the GoM, and the eastern boundary across the shelf of Nova Scotia.

The bathymetry of the model grid was populated by linearly interpolating the combined VDatum ADCIRC model grid bathymetry [17] and the bathymetry in the 2-min Gridded Global Relief Data (ETOPO2) [18]. Figure 2 displays the color coded bathymetry. The model grid resolves key bathymetric features such as Georges Bank, the Northeast Channel, the Great South Channel, etc.

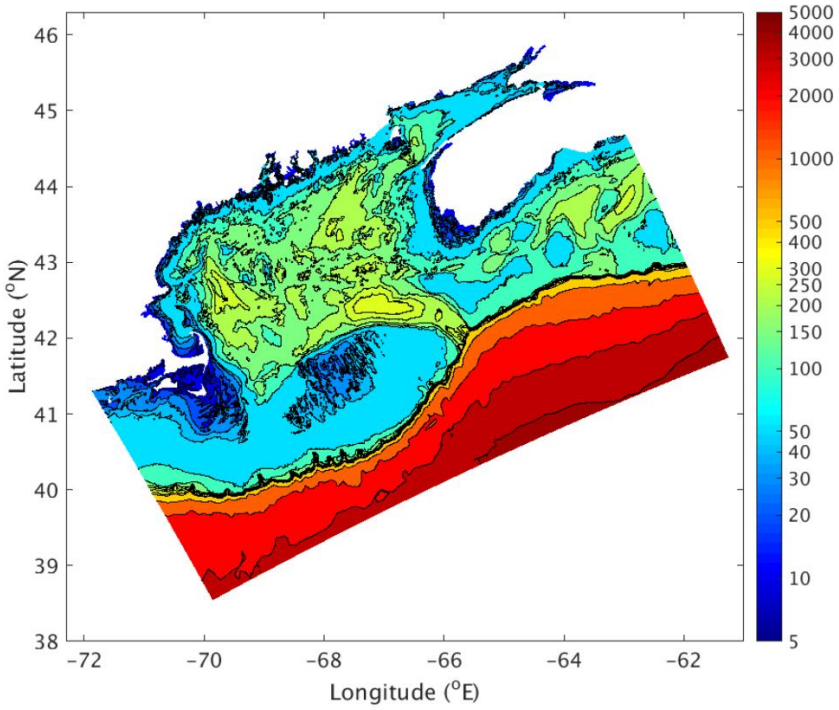

Figure 2. Bathymetry of the model grid. The color bar unit is meter.

The model is configured with 30 sigma layers. It uses the ROMS wetting and drying feature, a quadratic bottom friction scheme, and the two-equation model of the "revised" Mellor-Yamada Level 2.5 turbulence closure scheme (GLS/k-kl) implemented through the ROMS generic length scale (GLS) module.

For the open ocean boundary, we adopted the implicit Chapman condition for the free surface, the Flather condition for the 2-D momentum, and the radiation-nudging condition for the 3-D temperature, salinity, and velocity.

The hindcast simulation was driven with the complete suite of model forcing data including open ocean boundary forcing of the tidal and subtidal water level, 2-dimensional depth-averaged tidal currents, 3-dimensional temperature (T), salinity (S), and subtidal currents, river discharge, and the sea-surface meteorological forcing. It is noted that in the current setup the atmospheric pressure was not applied as a model forcing. Instead, we factored in the pressure effect by applying an inverse barometric pressure adjustment on the simulated water levels. In fact, we tested a setup with the air pressure forcing and the results appeared to be less satisfactory in terms of the model-data agreement.

The tidal water levels and currents on the open ocean boundaries were calculated using the tidal and currents harmonics of the TPXO 8.0-Atlas tidal database developed at the Oregon State University [19]. We chose eight tidal constituents (M_2, S_2, N_2, K_2, K_1, O_1, P_1, and Q_1) as the tidal forcing. The database was of the $1/30^\circ$ horizontal resolution and was interpolated onto the GoMOFS grid. Some adjustment on the tidal amplitude and phase along the model's open ocean boundary was made to optimize the model-data agreement at the water level stations. The adjustment was made through a trial-and-error procedure. In quantitative details, the amplitude was altered by -7.0 cm for M_2, -1.5 cm for S_2, -0.5 cm for N_2, 1.0 cm for P_1, and 3.0 cm for K_1; the phase was altered by

8.0 degrees for M_2, 2.0 degrees S_2, 6.0 degrees for N_2, 6.0 degrees for K_2, 8.0 degrees for P_1, and 10.0 degrees for K_1.

The non-tidal open ocean conditions used the nowcast results from the Global Real-Time Ocean Forecast System (G-RTOFS) [20,21]. The G-RTOFS is being operated by the NOAA National Centers for Environmental Prediction (NCEP). It is based on the Naval Oceanographic Office's configuration of the 1/12° eddy resolving global Hybrid Coordinates Ocean Model (HYCOM). Its ocean model has 4500 by 3298 horizontal dimensions and 32 vertical hybrid layers (isopycnals in the deep, isolevel in the mixed layer, and sigma in shallow waters). The system assimilates in situ profiles of temperature and salinity from a variety of sources and remotely sensed SST, SSH and sea-ice concentrations. The G-RTOFS is forced with 3-hourly momentum, radiation, and precipitation fluxes from the operational NCEP Global Forecast System. It runs once a day and produces nowcasts and forecast guidance for sea surface values (SSH, SST, and SSS) at three hour intervals, and full volume parameters (3-dimensional temperature, salinity, currents, and mixed layer depths) at six-hourly interval. The nowcast outputs of the three-hourly water level and the six-hourly 3-D currents and T/S as the non-tidal forcing were spatially interpolated onto the model grid's open ocean boundaries and temporally interpolated across the hindcast period of the entire year of 2012.

It is noted that no adjustment on the G-RTOFS data were performed to improve the accuracy of the open ocean boundary conditions. Due to the lack of real-time observations at locations along the GoMOFS open boundary, it is not feasible to realize the adjustment during the GoMOFS operational practice. Considering that the hindcast simulation with the non-adjusted G-RTOFS forcing demonstrated skills meeting the NOS standard skill assessment criteria (Section 5), we decided to accept the "flawed" model configurations and the results therein in the forecast implementation. It is noted that data assimilation should ultimately be the methodology (being considered for future NOS OFS implementations) to solve this kind of input errors.

The river forcing includes discharges from nine rivers along the Gulf coast. From north to south they are: St. John River, St. Croix, Machias River, Penobscot River, Kennebec River, Androscoggin River, Saco River, Merrimack River, and Neponset River. The river discharge and water temperature data were the U.S. Geological Survey (USGS) river discharge observations [22]. Note that the river discharge data were available at locations usually far from the river mouths. In the hindcast setup, the magnitude of the discharge was increased by 20%. This factor was determined through a series of empirical trial-and-error experiments.

The salinity was specified to be zero for all nine rivers. The assumption of zero salinity was the recourse that was decided upon after considering factors such as data availability, the model grid configuration for the river course, and the skill of the hindcast run results. The GoMOFS model grid goes into the river course by four to ten kilometers for different rivers rather than defining the river entrance by the nodes immediately along the open coast. The distances from the open coast are not large enough to fully justify the zero salinity assumption. However, there is a lack of salinity observations of the river discharge. Hence, following the "informal" common practice, we specified the zero salinity values rather than choosing any other arbitrary value. As an ad hoc justification for the zero-salinity assumption and for the adjusted discharge, the hindcast salinity demonstrated reasonably good agreement with the observations (Section 5).

The hindcast made use of the 12-km resolution forecast guidance of the NOAA National Center for Environmental Predictions (NCEP's) North American Mesoscale Forecast Modeling System (NAM) for surface forcing. The ROMS model was forced with 10-m wind velocity to compute the surface wind stress, 2-m surface air temperature and relative humidity, total shortwave radiation, downward longwave radiation, and the ROMS bulk formulation to calculate the air-sea momentum and heat fluxes, evaporation and precipitation rate to calculate the net salinity flux across the air-sea interface.

Two scenarios of model simulations were conducted: a tidal forcing only simulation and a hindcast simulation of year 2012. The model configuration in both simulations remains the same except that the former was initialized with constant water temperature and salinity and forced with

tidal water level and currents on the open ocean boundary, whereas the latter was driven with the total water level and currents on the open ocean boundary, sea-surface meteorological forcing, and river forcing. The purpose of the tidal only simulation was to verify the tidal open ocean boundary setup so as to ensure a favorable model performance in reproducing realistic water levels.

3. Observation Data

The observed data for the skill assessment are water levels from the NOS Center for Operational Oceanographic Products and Services (CO-OPS) water level stations, temperature (T) from the CO-OPS meteorological observation stations, the National Data Buoy Center (NDBC) buoys, and the Northeastern Regional Association of Coastal Ocean Observing Systems (NeraCOOS) buoys, and salinity (S) and currents from the NeraCOOS buoys.

The water level data in 2012 were downloaded from the NOS CO-OPS Web site [23]. Of the stations with the real time observations in 2012, the data from six stations (Figure 1a) were chosen for the model-data comparison by comparing the station location with the model domain and the grid layout. Some other stations located in the small estuaries, embayment, or inter-island channels which were not resolved by the model grid were excluded. They are the stations 8449130 (Nantucket Island, MA, USA), 8447930 (Woods Hole, MA, USA), 8447435 (Chatham, MA, USA), and 8410140 (Eastport, ME, USA).

The water temperature data were collected at five CO-OPS meteorological observation stations, ten NDBC buoys, and seven NeraCOOS buoys (Figure 1). All three data sets were downloaded from the NDBC online archive [24]. The CO-OPS and NDBC data were near surface observations. The depths of the CO-OPS and the NDBC measurements are shown in Figure 1a), respectively. The NeraCOOS measurement depths are listed in Table 1.

Table 1. Measurement depths of water temperature, salinity, and current velocity at the NeraCOOS buoys.

Station ID	Depth Relative to Mean Sea Level (m)		
	Temperature	Salinity	Current Velocity
A01	1, 2, 4 ,20, 50, 51	1, 20, 50	10, 22, 34, 46
B01	1, 2, 4, 20, 50	1, 20, 50	18, 30, 42
E01	1, 2, 4, 20, 50	1, 20, 50	18, 30, 42, 54, 66
F01	1, 2, 20	1, 20, 50	14, 26, 38, 50, 62, 74
I01	1, 2, 20, 50	1, 20, 50	14, 26, 38, 50, 62
M01	1, 2, 2.8, 20, 50, 150, 200	1, 20, 50, 200	34, 58, 82, 106, 130, 154, 178, 194
N01	1, 2, 20, 50, 100, 150,180	1, 20, 50, 100, 150, 180	24, 48, 72, 96, 104, 128, 152

Both the salinity and current velocity data were from the seven NeraCOOS buoys (Figure 1). Table 1 lists the corresponding measurement depths. The data were downloaded from the NeraCOOS website [25].

4. Results

4.1. Tidal Simulation

We computed the harmonic constants of tidal water levels using the outputs of the six-month, tidal forcing only simulation. Figure 3 displays the scatter plots of the model-data harmonics of four constituents: M_2, S_2, N_2, and K_1, respectively. The constituents represent the most prominent three semidiurnal and one diurnal constituents in the area. Table 2 lists the corresponding station IDs and the model-data differences at 24 NOS/CO-OPS water level stations encompassed in the GoMOFS domain.

For all the four constituents, the model-data discrepancy lies within the ten-percent lines at nearly all stations. A further detailed investigation indicated that the few outliers (see plots in Figure 3c,e,g,h)

correspond to some coastal locations which were barely resolved with the current model grid. Over the 24 stations, the averaged root-mean-squared errors (RMSE) of the tidal amplitude are 4.3, 1.6, 1.7, 0.8 cm for M_2, S_2, N_2, and K_1, respectively; the corresponding RMSEs for tide phase are 3.8, 7.3, 4.5, and 3.3 degrees. Note that in obtaining the K_1 phase error of 3.3 degrees, three outlier stations (8455083, 8459338, and 8459479) were excluded from the calculation.

In general, the tidal simulation produced favorable model-data agreement with respect to both amplitude and phase. This helps the hindcast and the future nowcast/forecast system to reproduce realistic water levels.

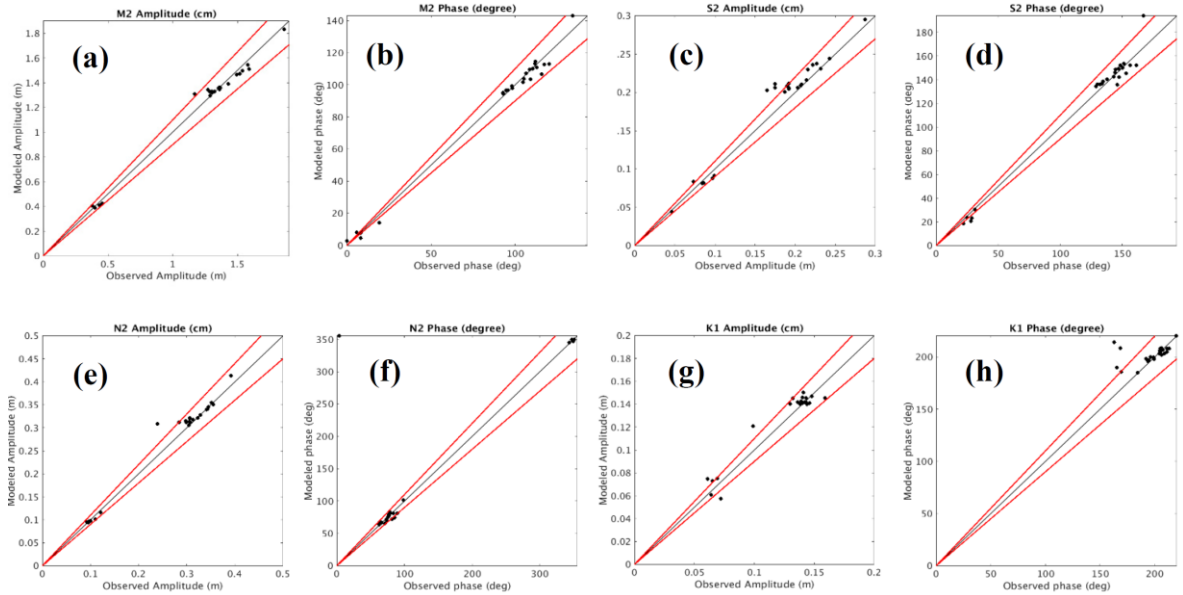

Figure 3. Scatter plots of the tidal harmonic constants (amplitudes and phases) of M_2, N_2, S_2, and K_1 constituents between model results and observations. The red lines on each plot outline the ten percent deviation from the perfect model-data match. (**a**) M_2 amplitude; (**b**) M_2 phase; (**c**) S_2 amplitude; (**d**) S_2 phase; (**e**) N_2 amplitude; (**f**) N_2 phase; (**g**) K_1 amplitude; and (**h**) K_1 phase.

4.2. Hindcast Simulation

The hindcast simulation ran from 1 January to 30 December 2012. It started from a still water state with the T/S fields initialized with the G-RTOFS results. Following an initial 5-day ramping up, the model run continued for another 10 days to ensure that an equilibrium state was reached. The time series of the ocean state variable (water level, currents, and T/S) were recorded at the 6-min interval from the 15th day to the end of the hindcast run. We then used the time series to evaluate the model performance using the NOS standard skill assessment software [16].

4.2.1. Water Levels

Figure 4 showed both the modeled and observed subtidal water level time series after applying a 30-day Fourier Transform low-pass filter to the total water level data. The model results demonstrated favorable agreement with the observations during both the event-free period (October) and the event period (early November). For instance, the model successfully reproduced the water level setup at stations 8423898, and 8443970 in early November (Figure 4e,f). At some stations, such as 8419317 and 8423898 (Figure 3d,e), the model slightly over-predicted the water levels in mid-October.

Table 2. The model-data comparison of harmonic constants for the M_2, S_2, N_2, and K_1 constituents, respectively. The stations are listed in the order of the total tidal range ranking from the largest to the smallest.

Station ID	Station Name	Differences between the Model Predictions and Observations							
		M_2 amp (cm)	M_2 Phase (Degree)	S_2 amp (cm)	S_2 Phase (Degree)	N_2 amp (cm)	N_2 Phase (Degree)	K_1 amp (cm)	K_1 Phase (Degree)
8411250	Cutler Naval Base, ME	−2.7	2.1	0.8	6.3	2.1	1.3	0.9	−2.7
8414721	Fort Pt., ME	−7.6	1.2	1	4	−0.5	4.4	−0.1	−7.6
8413320	Bar Harbor, ME	−3.4	1.7	0.1	5.5	0.3	1.1	0.6	−3.4
8413825	Mackerel Cove, ME	−4.1	1	1.4	3.9	0	−5.9	−1.4	−4.1
8414249	Oceanville, Deer Isle, ME	−4.5	2	−0.1	−10	−0.1	2.7	1.3	−4.5
8414888	Penobscot Bay, ME	−2.7	−0.5	1.4	3	−0.2	0	0.3	−2.7
8447241	Sesuit Harbor, MA	−3.9	1.4	0.2	3.9	0	2.1	0.4	−3.9
8446121	Provincetown, MA	−0.7	2.5	3.6	2.5	−0.2	3.7	0.6	−0.7
8446166	Duxbury Harbor, MA	0.2	−7.3	2	−9.1	1.6	−8.4	0	0.2
8444525	Nut Island, MA	−1.3	−0.5	0.2	2.1	0.5	1	0.2	−1.3
8446493	Plymouth Harbor, MA	0.2	−4.6	0.3	−4.3	1.4	−2.7	0.2	0.2
8444162	Boston Light, MA	0.6	0.9	0.3	4.1	0.8	0.5	0.2	0.6
8418606	Saco River, ME	2.5	−1.5	1.4	−0.6	1.3	−1.5	−0.5	2.5
8446009	Green Harbor River, MA	1.9	−1.9	1.3	−0.2	0.5	1.8	0.2	1.9
8441551	Rockport Harbor, MA	0.8	0.7	1.3	2	0.2	−0.1	−0.4	0.8
8418445	Pine Point, ME	4.6	−5.5	3.1	−5.2	2.8	−9.7	0.1	4.6
8417177	Hunniwell, ME	7.1	−3	1.9	2.9	1.7	−3.4	−0.1	7.1
8440452	Plum Island, MA	14.1	−9.1	3.8	−7.6	7	−10.9	1	14.1
8455083	Point Judith, RI	−3.3	−3.7	−0.8	−7.5	−0.9	−2.6	−0.3	−3.3
8447605	Hyannisport, MA	−3.1	8.8	−0.2	26.9	−0.5	2.4	2.2	−3.1
8459338	Block Island, RI	−2.5	−357	−0.9	−3.5	−0.2	1.7	1.4	−2.5
8459681	Block Island, RI	−0.8	2.2	−0.3	−1.4	−0.1	2.6	0.8	−0.8
8459479	Sandy Point, RI	−0.5	−0.5	−0.4	−5.6	0.1	−0.8	0.6	−0.5
8458022	Block Island Sound, RI	2.6	−5.3	1	−0.7	0	351.6	−1.4	2.6

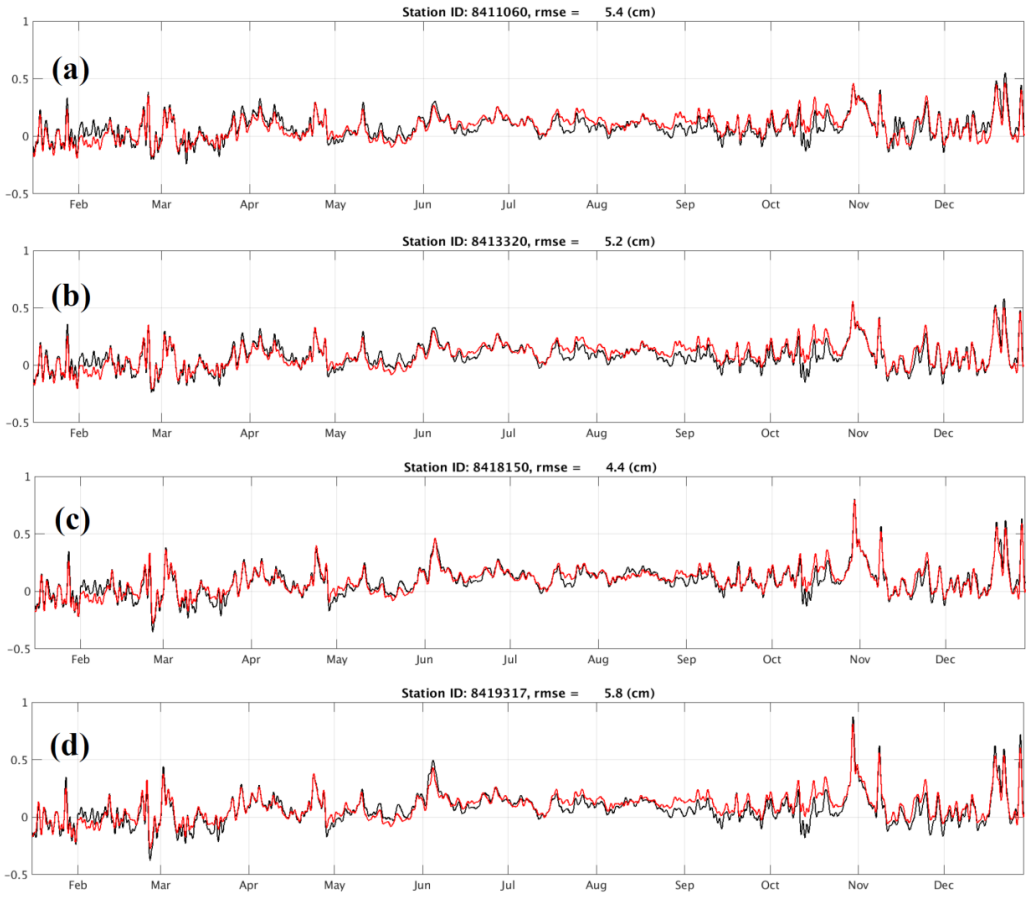

Figure 4. *Cont.*

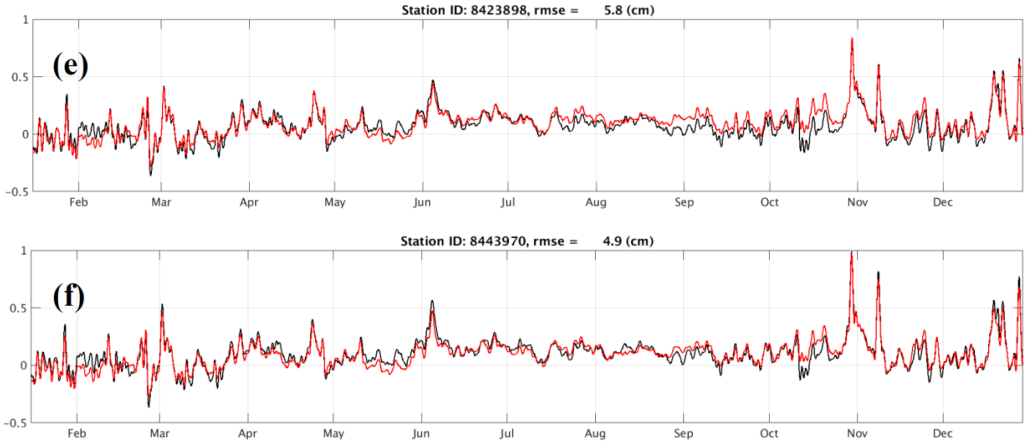

Figure 4. Subtidal water levels at six CO-OPS water level stations (Figure 1). The red and black lines represent the model results and observations, respectively. The six plots are for stations (**a**) 8411060; (**b**) 8413320; (**c**) 8418150; (**d**) 8419317; (**e**) 8423898; and (**f**) 8443970.

4.2.2. Currents

Figure 5 displays the (u, v) components of the modeled and observed subtidal time series at three measurement depths (10 m, 22 m, and 46 m) at buoy A. The subtidal data were extracted from filtering the model output with a 30-h low-pass Fourier filter.

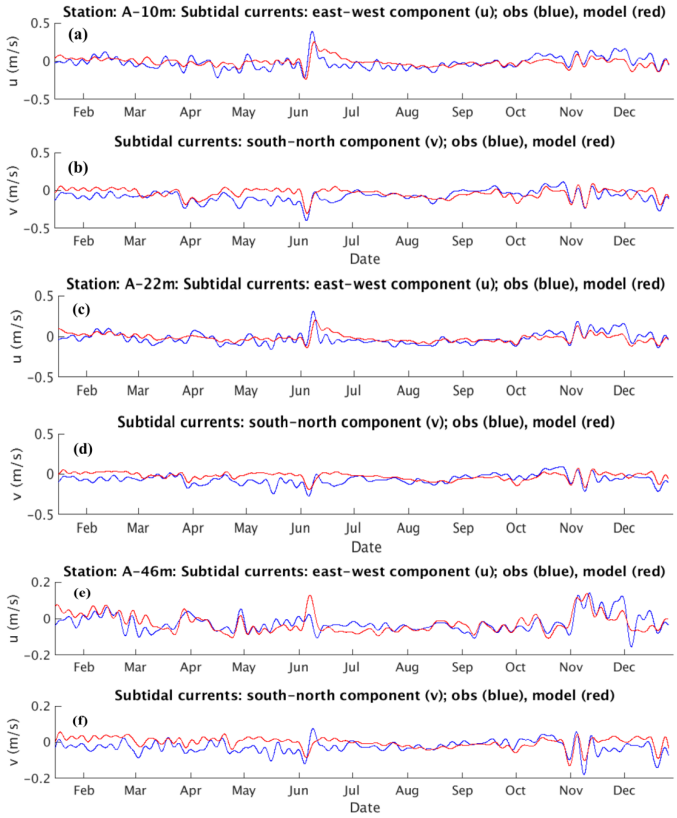

Figure 5. Comparison of the model (red lines) and the data (blue lines) time series of the current velocity (u, v) at the NeraCOOS buoy station A. The measurement depths are shown on the plots. (**a**,**b**) depict the u and v components at the 10 m depth; (**c**,**d**) depict the u and v components at the 22 m depth; and (**e**,**f**) depict the u and v components at the 46 m depth.

The hindcast simulation successful reproduced in the events taking place in early June and early to mid-November, respectively. During the events, the currents appeared to be more intense in shallow layers (at 10 m and 22 m) than in deeper layers (at 46 m). Comparison of the time series between the winds and the currents indicated that the enhanced currents speeds resulted from the intensified wind stress during the events.

4.2.3. Water Temperature

The modeled temperature time series were compared with the observations at the CO-OPS meteorological stations and the NDBC buoys, and NeraCOOS buoys. The model results demonstrate favorable agreement with the observations. As an example, the left panel in Figure 6 displays the monthly averaged temperature at six depths (1 m, 20 m, 50 m, 100 m, 150 m, and 200 m) at the NeraCOOS buoy M01. The plots illustrated that the model successfully reproduced both the magnitude and the annual cycle of the temperature. The near surface water temperature varied between 6 °C in the winter and the early spring and 20 °C in the mid-summer. In deeper water, temperature remained at a nearly constant value of 9 °C throughout the year. This suggests that an intense thermocline existed during the summer and completely faded away in the winter.

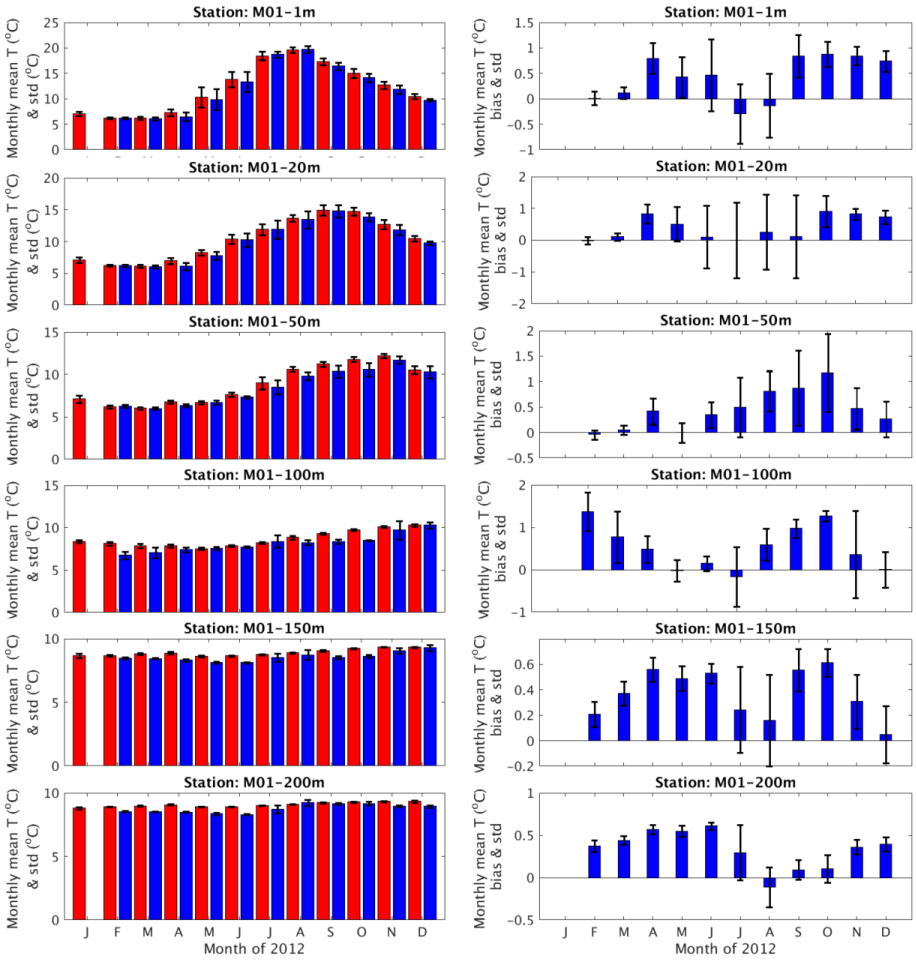

Figure 6. (**Left panel**) Comparison of the monthly averaged water temperature between the model (red bars) and the observations (blue bars) at the NeraCOOS buoy M01. The measurement depths are as shown on each plot. On some plots the observations do not appear due to the lack of data. (**Right panel**) Bias of the modeled monthly mean temperature. The thin lines on top of each bar plot represent the corresponding standard deviations.

The right panel in the figure displays the bias and the standard deviation (std) of the monthly averaged model temperature. The bias ranged from near zero to less than 1 °C and did not exhibit evident trend of seasonal variations. The std ranged between 0.03 and 1.2 °C and appeared to be greater in summer than in spring and winter.

4.2.4. Salinity

The modeled time series were compared with observations at the seven NeraCOOS buoys (Figure 1 and Table 1). The left panel in Figure 7 displays the monthly averaged salinity of at buoys A01 and M01. The corresponding measurement depths were 1 m, 20 m, and 50 m at buoy A01 and 1 m, 20 m, 50 m, 100 m, 150 m, and 200 m at buoy M01. The right panel displays the corresponding model bias and std.

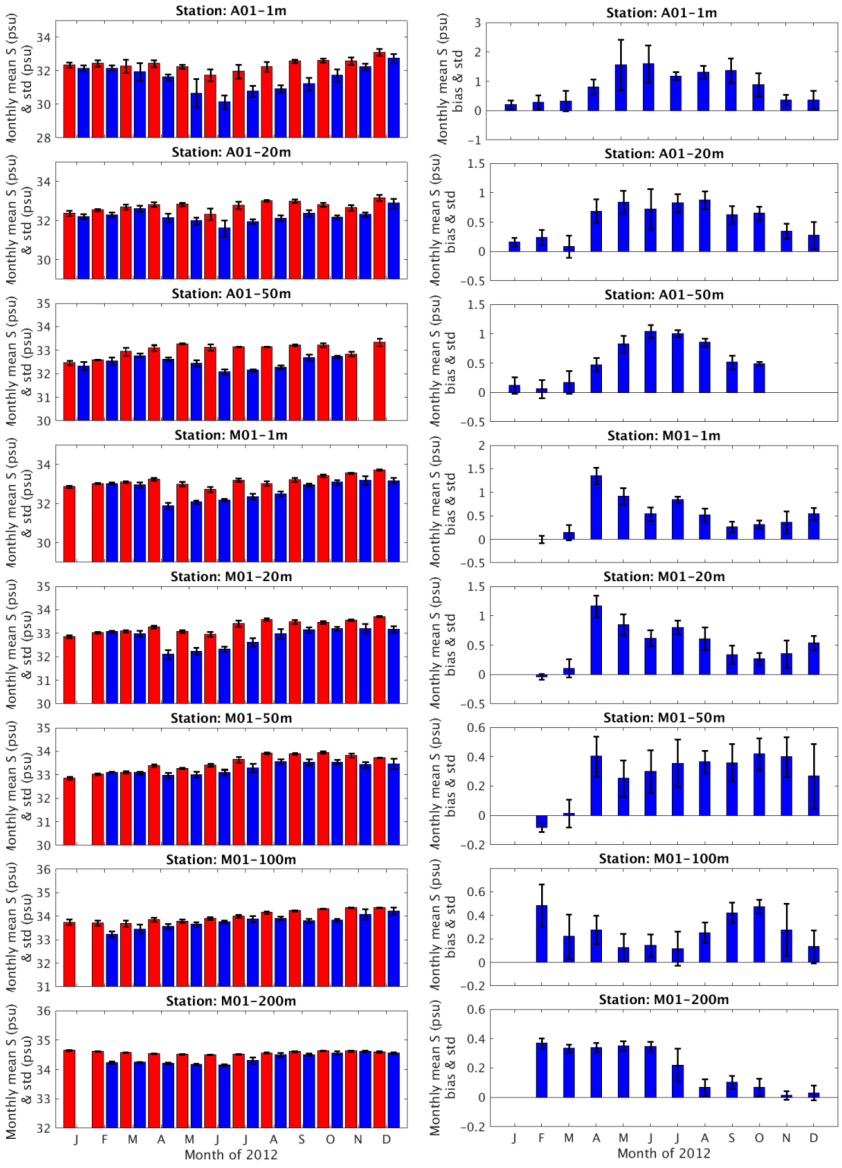

Figure 7. (**Left panel**) Comparison of the monthly averaged salinity between the model (red bars) and the observations (blue bars) at the NeraCOOS buoys A01 and M01. The station name and the measurement depths are as shown on each plot. On some plots the observations do not appear due to the lack of data. (**Right panel**) Bias of the modeled monthly mean temperature. The black lines on top each bar represent the corresponding standard deviations.

In general, salinity exhibited greater temporal variability near the surface than in deeper waters, especially during the late spring, summer, and early fall. The modeled salinity demonstrated positive biases with the typical magnitude of 0.5–1.0 psu at nearly each station throughout the year. This indicated that the hindcast tended to overestimate the salinity. However, this did not seem to be rooted from the specifics of the currently adopted turbulence closure scheme (TCS). In fact, the other TCS such as the k-ε, k-ω, and KPP models in the ROMS were also tested and they demonstrated similar model skills. Model bias might be attributed to inherent errors of various model forcing data.

During these periods, the model-data discrepancy appeared to be greater than in the winter. For instance, at buoy A01 the modeled surface salinity differed from the observations by 1.5 to 2 psu in the summer months, whereas the two exhibited close match in the winter months. Farther offshore at buoy M01, the model-data discrepancy appeared to be much smaller than at buoy A. The model agreed well with the observations in the fall and winter seasons. Even during the hydrodynamically active spring and summer seasons, the model-data differed by less than about 1 psu.

To examine the impact of the river discharges and rainfall forcings on the modeled salinity, we estimated the correlation coefficient, C_{SP}, between the sea-surface salinity (SSS) and the precipitation rate and the coefficient, and C_{SR} between the SSS and the discharge rates from the nearest river to each NeraCOOS station. It was found that the magnitude of C_{SP} was less than 0.06 at all stations. This seems to indicate that at the NeraCOOS stations the rainfall played a minor role in determining the modeled SSS compared with other forcing factors or ambient conditions.

C_{SR} was -0.42 and -0.46 at Stations B and F, respectively and was much less significant ($|C_{SR}| < 0.05$) at the other stations. Note that Stations B and F are relatively closer to the river entrance than the others and therefore demonstrated relatively higher C_{SR}. Figure 8a,b display the SSS and river discharge time series at Stations B and F to highlight the close correlation between the two properties at the stations.

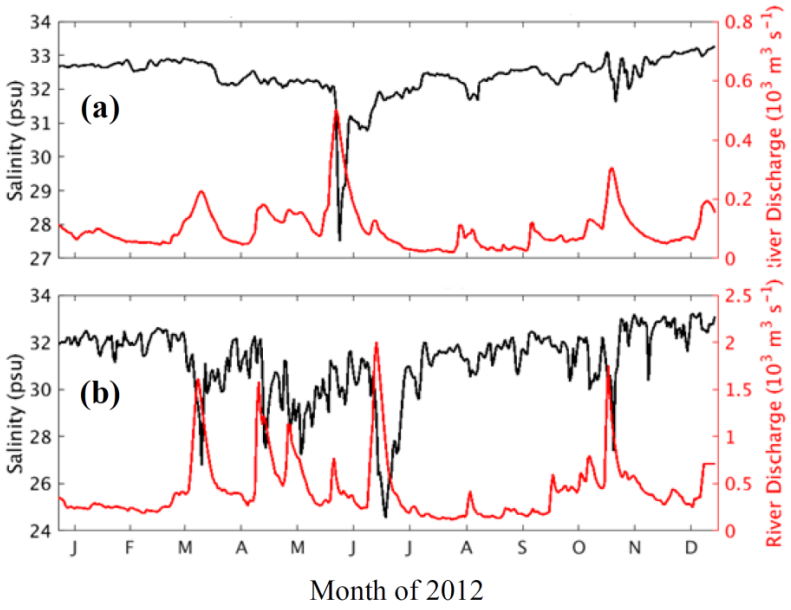

Figure 8. Daily time series of salinity (S) (black lines) and the river discharge (Q) (red lines): (**a**) S at station B01 vs. Q of the Saco River and (**b**) S at Station F01 vs. Q of the Penobscot river.

5. Skill Assessment

We evaluated the hindcast results using the NOS standard skill assessment software [16]. The model time series of water level, currents, temperature, and salinity were compared against the observed data (Section 2). In the following, we focused on reporting two key parameters, RMSE and the central frequency (CF). CF represents the fraction (percentage) of the model errors that are less

than some prescribed criteria of RMSE. The NOS standard prescribes the criteria as 0.15 cm for water level, 0.26 m/s for the currents speed and 22.5 degree for the phase of currents, 3.0 °C for temperature, and 3.5 psu for salinity, as well as the constant value of CF equal to 90% for all the above ocean state parameters. The present skill assessment results demonstrated that the hindcast performance met the above criteria. It is noted that the one set value criteria are not region specific and may not reflect the regional variability of the concerned variables. Hence it poses limitations on the validity and applicability of the model skill metrics from the criteria.

We compared the criteria with the performance of the nowcast/forecast system of the Gulf of Maine Ocean Observing System (GoMOOS) [10] in terms of monthly averaged properties (i.e., T, S, and current speeds). In general, the GoMOOS model skill in all three variables meet the NOS criteria, especially for the 3 °C RMSE temperature criteria. The present results (reported in the following) also meet the criteria with large margins at nearly all stations. In this regard, the 3 °C criteria does not pose serious change to the model skill in the GoM region. This seems to indicate that the region specific criteria would be needed to closely reflect the model skill. Bearing this in mind, we adopted the constant criteria in this study before any regional dependent criteria are officially developed in the future.

5.1. Water Level

Figure 9 display the model RMSE and CF, respectively. The RMSE ranges nearly from 0.09 m (Station ID 8418150, Portland, ME, USA) to 0.13 m (Station ID 8411060, Cutler Farris Wharf, ME, USA). The CF ranges from 76.2% (Station ID 8411060, Cutler Farris Wharf, ME) to 89.6% (Station ID 8418150, Portland, ME, USA). With respect to the RMSE and CF, the hindcast demonstrated better skill at stations near the central western Gulf coast than that along the Massachusetts coast and the northern Maine coast.

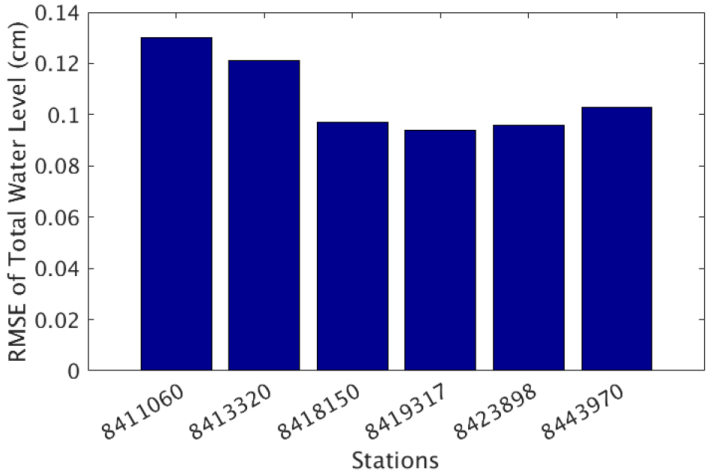

Figure 9. RMSE of the modeled water level.

The better model skill in the central domain stations might be attributed to their particular geographical locations. The stations are farther away from either the open ocean boundary (OOB) or the Bay of Fundy (BF) area compared with the other stations. The tidal range in the BF may reach up to nearly 7 m due to the tidal resonance effect (Section 1). The farther distance naturally made the central domain receive less adverse impact on the model skill due to the inherent inaccuracies in the OOB conditions or the errors in the model predicted tidal resonance effect in the BF.

5.2. Currents

Figure 10a,b displays the RMSE the currents speed and phase, respectively. In each figure, the station ID is named with the first letter denoting the buoy ID (Figure 1) and the following digits denoting the measurement depths in meter.

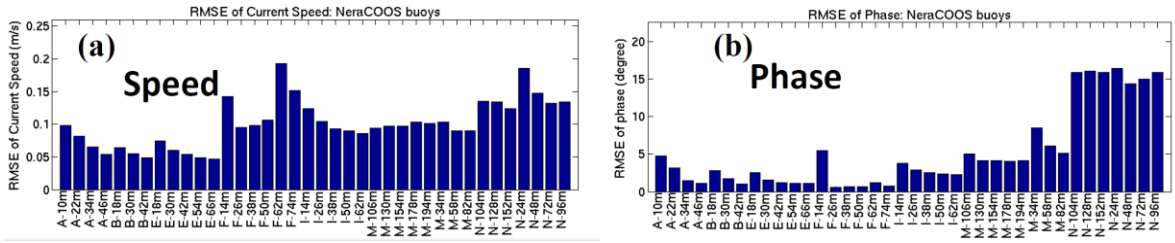

Figure 10. Skill assessment results of the currents speed and phase. (**a**) RMSE of speed and (**b**) RMSE of phase.

For the current speed, the RMSE ranges from 0.05 m/s at station E-66m to about 0.20 m/s at stations F-74m and N-24m. CF were mostly greater than 95% and lay between 80% and 90% at stations F-74m and N-24m. At buoys stations A, B, E, F, and M, RMSEs ranged between less than 2 degrees to 10 degrees and CFs were all above 95%. At station N01, RMSE was between 15 cm/s and 17 cm/s and CF was around 85% at all depths.

Note that the station N01 demonstrated significantly less favorable model skills than the other stations. This might be related to the complex hydrodynamics in the Northeast Channel where the station is located (Figure 1a). The channel has a sill depth of 230 m and is the major pathway for the water mass exchange between the Gulf and the open ocean. The deep ocean water flows into the central Gulf at depths and the Scotian water flows across the channel in the near surface layer. The channel also serves as a major route for tidal energy to propagate into the Gulf. The combined subtidal and tidal currents may reach a speed of 1 m/s or more. In contrast, hydrodynamics in the other areas of the Gulf appear to be much less complex. The complex hydrodynamics in the channel posed more serious challenges to realistically reproduce the local hydrography than elsewhere and contributed to the greater model errors at Station N01.

5.3. Water Temperature

Figure 11 illustrates the skill assessment results in three groups with respect to the sources of observed data, i.e., CO-OPS stations, the NDBC buoys, and the NeraCOOS buoys. In each figure, the abscissa represents the station ID. In particular, the NeraCOOS station IDs (Figure 11c) followed the same naming convention as shown in Figure 8. Both the CO-OPS and the NDBC buoy data corresponded to the near surface measurements and the NeraCOOS data correspond to both the surface and in-depth measurements. In addition, the CO-OPS stations are located in the nearshore area whereas the other two data sets (the NDBC and NeraCOOS buoys) correspond to the further offshore areas and even in the central Gulf and near the shelfbreak area. Therefore, the skill assessment results of the three groups represent the hindcast performance in different hydrodynamic regimes, e.g., nearshore vs. offshore areas as well as at the sea surface vs. the in-depth waters.

The RMSE at the seven CO-OPS stations ranged from 0.9 °C to 1.7 °C and CF was all above 95%. The RMSE at the NDBC stations was between 0.7 °C and 1.8 °C. Correspondingly CF was above 90%.

The RMSE at the NeraCOOS stations ranged from less than 1.0 °C at station M01 in the eastern Gulf to around 2.3 °C at stations N01-20m and −50 m. CF was above 90% except at stations N01-20m and −50 m for which CF equaled ~80%. Note that buoy N is located in the Northeast Channel (Figure 1).

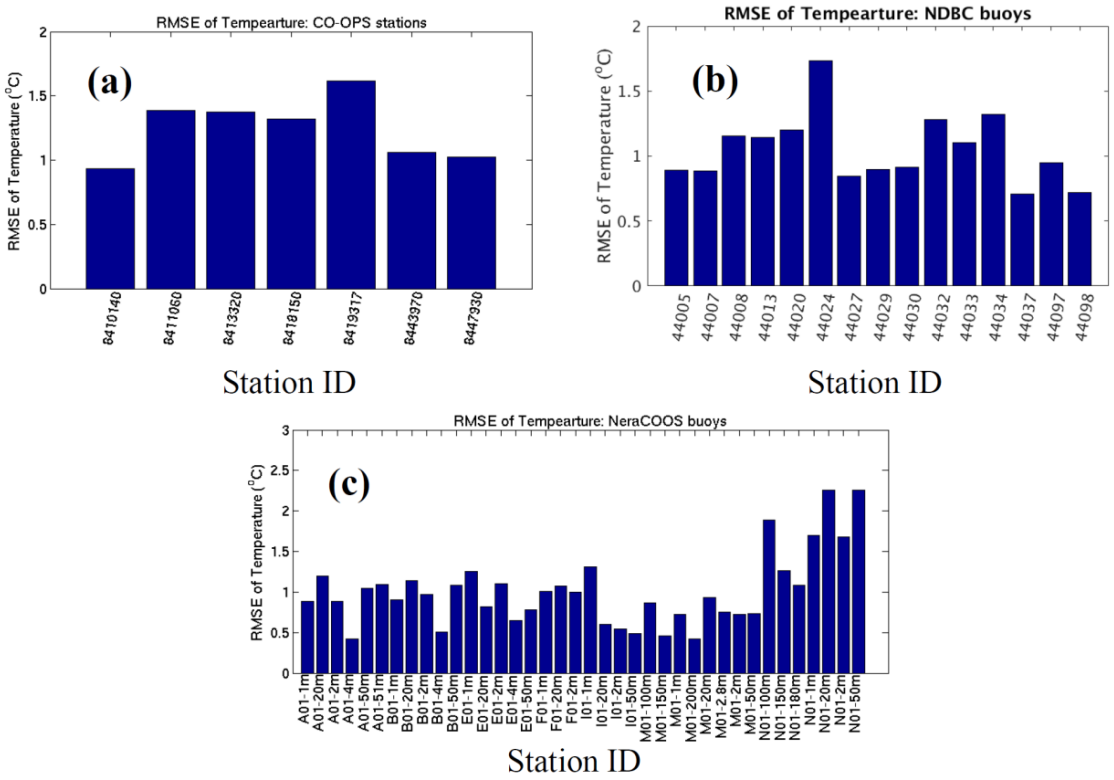

Figure 11. The RMSE of the modeled water temperature compared with three sets of observed data, (**a**) the CO-OPS stations; (**b**) the NDBC buoys; and (**c**) the NeraCOOS buoys.

5.4. Salinity

Figure 12 displays the RMSE of the salinity skill assessment results. In general, the RMSE ranged from 0.2 psu to 1.5 psu and the CF was close to 100%. At buoys A, B, E, F, I, and M, the RMSE of the near-surface salinity was around 1.0–1.5 psu, whereas the RMSE in the subsurface layer is much smaller, less than 0.7 pus in general. At buoy N, the RMSEs at all three depths (1 m, 20m, and 50 m) were between 1.0 psu and 1.4 psu.

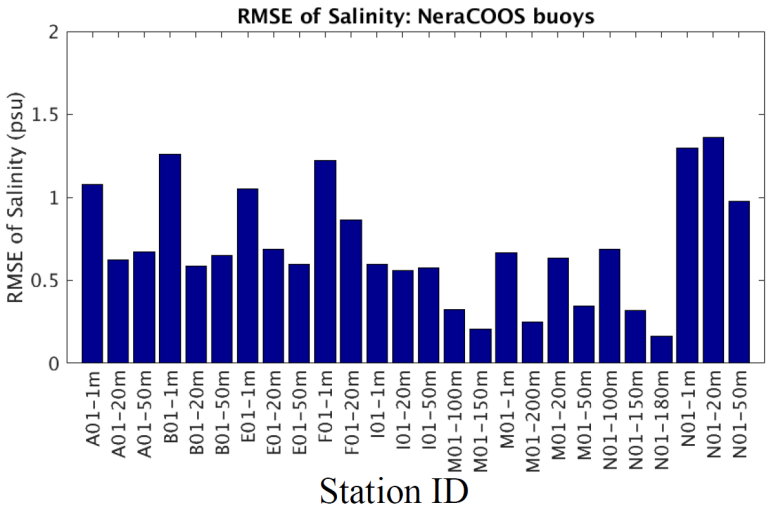

Figure 12. The RMSE of the modeled salinity.

6. Summary and Conclusions

The NOAA NOS is developing the Gulf of Maine operational nowcast/forecast system (GoMOFS) to aim for producing real-time nowcast and short-range forecast guidance for water levels, 3-dimensional currents, water temperature, and salinity over the broad GoM region. Following the routine procedure of the OFS development, we conducted a one-year period hindcast simulation of 2012. This manuscript described the model development, hindcast setup and the skill assessment results.

The model performance was evaluated using the NOS standard skill assessment software and the criteria by comparing the hindcast results with the observed time series of water level, T/S, and currents collected by both the NOAA agencies (including the CO-OPS and NDBC) and the NeraCOOS. In general, the hindcast results met the skill assessment criteria. The RMSE was about 0.12 m for water level, less than 1.5 °C for temperature, less than 1.5 psu for salinity, and less than 0.2 m/s for the currents speed and less than 15 degrees for the currents phase. The corresponding central frequency was between 80% and 90% for the water level and generally above 90% for the other properties.

The NOS is working on transitioning the hindcast setup into operations on the NOAA's Weather and Climate Operational Supercomputing System. The GoMOFS is anticipated to be in operations in fiscal year 2017.

Acknowledgments: John Wilkin, Hernan G. Arango, Julia Levin, Javier Zavala-Garay at the Rutgers University, Ruoying He at the North Carolina State University, and Dennis McGillicuddy at Woods Hole Oceanographic Institution provided valuable comments and data supports on the GoMOFS development. Three anonymous reviewers provided insightful comments and suggestions that substantially improved this paper. The authors would like to express our sincere gratitude for their help.

Author Contributions: All the authors contributed to the system development. Z.Y. conducted the hindcast simulation and the skill assessment.

Conflicts of Interest: The authors declare no conflicts of interest.

References

1. Chen, C.; Beardsley, R.C. Tidal mixing over a finite amplitude asymmetric bank: A model study with application to Georges Bank. *J. Mar. Res.* **1998**, *56*, 1163–1201. [CrossRef]
2. Chen, C.; Beardsley, R.C. A numerical study of stratified tidal rectification over finite-amplitude banks. Part I: Symmetric bank. *J. Phys. Oceanogr.* **1995**, *25*, 2090–2110. [CrossRef]
3. Naimie, C.E. Georges Bank residual circulation during weak and strong stratification periods: Prognostic numerical model results. *J. Geophys. Res.* **1996**, *101*, 6469–6486. [CrossRef]
4. Naimie, C.E.; Loder, J.W.; Lynch, D.R. Seasonal variation of the three-dimensional residual circulation on Georges Bank. *J. Geophys. Res.* **1994**, *99*, 15967–15989. [CrossRef]
5. Xue, H.; Chai, F.; Perrigrew, N.R. A model study of the seasonal circulation in the Gulf of Maine. *J. Phys. Oceanogr.* **2000**, *30*, 1111–1135. [CrossRef]
6. Wiebe, P.; Beardsley, R.; Mountain, D.; Bucklin, A. U.S. Globec Northwest Atlantic/Georges Bank program. *Oceanography* **2003**, *15*, 13–29. [CrossRef]
7. Zhang, A.; Wei, E.; Parker, B.B. Optimal estimation of tidal open boundary conditions using predicted tides and adjoint data assimilation technique. *Cont. Shelf Res.* **2003**, *23*, 1055–1070. [CrossRef]
8. Greenberg, D.A. Modeling the mean barotropic circulation in the Bay of Fundy and Gulf of Maine. *J. Phys. Oceanogr.* **1983**, *13*, 886–904. [CrossRef]
9. Chen, C.; Beardsley, R.C.; Franks, P.J.S. A 3-D prognostic model study of the ecosystem over Georges Bank and adjacent coastal regions. Part I: Physical model. *Deep Sea Res.* **2001**, *48*, 419–456. [CrossRef]
10. Xue, H.; Shi, L.; Cousins, S.; Pettigrew, N.R. The GoMOOS nowcast/forecast system. *Cont. Shelf Res.* **2005**, *25*, 2122–2146. [CrossRef]
11. Yang, Z.; Myers, E. Barotropic Tidal Energetics and Tidal Datums in the Gulf of Maine and Georges Bank Region. In *Estuarine and Coastal Modeling, American Society of Civil Engineers*, Proceedings of the 10th International Conference, Newport, RI, USA, 10–12 November 2007; Spaulding, M.L., Ed.; 2007; pp. 74–94.

12. Chen, C.; Huang, H.; Beardsley, R.C.; Xu, Q.; Limeburner, R.; Cowles, G.W.; Sun, Y.; Qi, J.; Lin, H. Tidal dynamics in the Gulf of Maine and New England Shelf: An application of FVCOM. *J. Geophys. Res.* **2011**, *116*, C12010. [CrossRef]
13. Gangopadhyay, A.; Robinson, A.R.; Haley, P.J., Jr.; Leslie, W.G.; Lozano, C.J.; Bisagni, J.J.; Yu, Z. Feature oriented regional modeling and simulations (FORMS) in the Gulf of Maine and Georges Bank. *Cont. Shelf Res.* **2003**, *23*, 317–353. [CrossRef]
14. Wilkin, J.; Levin, J.; Zavala-Garay, J.; Arango, H.; Hunter, E.; Robertson, D.; Fleming, N. ROMS 4DVar Data Assimilation: Mid-Atlantic Bight and Gulf of Maine. Available online: http://maracoos.org/sites/macoora/files/downloads/Wilkin-Rutgers-OMG.pptx (accessed on 8 July 2016).
15. Shchepetkin, A.F.; McWilliams, J.C. The Regional Ocean Modeling System: A split-explicit, free-surface, topography following coordinates ocean model. *Ocean Model.* **2005**, *9*, 347–404. [CrossRef]
16. Zhang, A.; Hess, K.W.; Wei, E.; Myers, E. *Implementation of Model Skill Assessment Software for Water Level and Current*; NOAA Technical Report NOS CS 24; U.S. Department of Commerce, National Oceanic and Atmospheric Administration: Silver Spring, MA, USA, 2006; p. 61.
17. Yang, Z.; Myers, E.P.; Jeong, I.; White, S.A. *VDatum for the Gulf of Maine: Tidal Datums, Marine Grids, and Sea Surface Topography*; NOAA Technical Memorandum NOS CS 31; U.S. Department of Commerce, National Oceanic and Atmospheric Administration: Silver Spring, MA, USA, 2013; p. 50.
18. National Geophysical Data Center (NGDC). 2-Minute Gridded Global Relief Data (ETOPO2v2). Available online: https://www.ngdc.noaa.gov/mgg/global/etopo2.html (accessed on 28 October 2016).
19. Egber, G.; Erofeeva, L. Efficient Inverse Modeling of Barotropic Ocean Tides. *J. Atmos. Oceanic Technol.* **2002**, *19*, 183204.
20. Mehra, A.; Rivin, I.; Garraffo, Z.; Rajan, B. Upgrade of the Operational Global Real Time Ocean Forecast System. Available online: https://www.wcrp-climate.org/WGNE/BlueBook/2015/individual-articles/08_Mehra_Avichal_etal_RTOFS_Upgrade.pdf (accessed on 29 October 2016).
21. Garaffo, Z.D.; Kim, H.-C.; Mehra, A.; Spindler, T.; Rivin, I.; Tolman, H.L. Modeling of ^{137}Cs as a tracer in a regional model for the Western Pacific, after the Fukushina-Daiichi Nuclear power plant accident of March 2011. *Weather Forecast.* **2016**, *21*, 553–579. [CrossRef]
22. U.S. Geological Survey (USGS). USGS Water Data for the Nation. Available online: http://waterdata.usgs.gov/nwis/ (accessed on 15 October 2013).
23. Center for Operational Oceanographic Products and Services (CO-OP). Water Levels—Station Selection. Available online: http://tidesandcurrents.noaa.gov/stations.html?type=Water+Levels (accessed on 28 October 2016).
24. National Data Buoy Center (NDBC). Archive of Historical Ocean Data. Available online: http://www.ndbc.noaa.gov/data/historical/ocean/ (accessed on 28 October 2016).
25. Northeastern Regional Association of Coastal Ocean Observing Systems (NeraCOOS). Graphing and Download. Available online: http://neracoos.org/datatools/historical/graphing_download (accessed on 28 October 2016).